SPATIALLY AND CONDUCTIVITY LOG CONSTRAINED AEM INVERSION

Ross C Brodie
Geoscience Australia
GPO Box 378, Canberra, ACT, 2601
Ross.C.Brodie@ga.gov.au

*Yusen Ley-Cooper
Geoscience Australia
GPO Box 378, Canberra, ACT, 2601
Yusen.LeyCooper@ga.gov.au

SUMMARY

We have developed an algorithm and released open-source code for 1D inversion of airborne electromagnetic data incorporating spatial and conductivity log constraints. The deterministic gradient based inversion algorithm uses an all-at-once approach, in which whole datasets or flight lines are inverted simultaneously. This allows spatial constraints to be imposed while also ensuring the inversion model closely matches any downhole conductivity logs that are near to the flight lines. The intent of the algorithm is to improve consistency along and across flight lines by taking advantage of the assumed coherency of the geology.

Instead of roughness constraints, 'sameness' constraints are used. To implement these the regularization penalizes differences between the conductivity of 1D model/layer pairs and the weighted average conductivity of every other neighbouring 1D model within a user selected radius of their position. The neighbour averages are computed with inverse distance to a power weighting. The comparisons can be made over equivalent elevations. Downhole conductivity log constraints are imposed in a similar fashion, by penalizing the differences between conductivity logs, averaged over selected intervals, with their respective neighbouring 1D models. Overall the regularization encourages the final 1D conductivity models to be as similar as possible to their neighbours and to conductivity logs.

It is demonstrated with an example that the method enhances geological interpretation by improving the model's continuity along and between flight lines, and its match to conductivity logs.

Key words: AEM, airborne, electromagnetic, inversion, constrained, conductivity log.

INTRODUCTION

Conductivity models derived from layered earth, or one dimensional (1D) inversion of airborne electromagnetic (AEM) data often exhibit some degree of incoherency when displayed as depth-sections or imaged grids of depth slices. This can particularly be the case for conventional, so called 'stitched', 1D inversion where each AEM sounding (or sample) is inverted totally independently of all other soundings and then later stitched into a combined model. The incoherence stems from noise in the data coupled with the fundamental non-uniqueness of the geophysical inversion process. Increased noise in adjacent soundings results in, sometimes large, differences in adjacent conductivity models, leading to conductivity sections that are somewhat vertically striped, or have artefacts at depth.

When each sounding is inverted independently there is no opportunity to take advantage of the fact that adjacent conductivity models should be correlated at the same lateral scale length as the geology (subsurface conductivity). Furthermore, when inverting soundings independently, there is no obvious way to incorporate constraints from downhole conductivity log data from boreholes that may be located throughout the survey area. Certainly, if a borehole conductivity log is coincident with, or close enough to, a particular sounding it can be used as an a priori constraint, but this will not be the case in general. Typically one has to resort to using softer constraints based on a laterally-constant reference model by averaging conductivity logs over the whole, or some portion, of the survey area (e.g., Lane *et al.*, 2004).

One way to make use of the assumed lateral continuity of the geology, and hence the conductivity, and to also incorporate borehole conductivity log data is to invert some or all of the AEM soundings at once. By doing this some form of lateral constraint can be imposed between neighbouring soundings. Also constraints can be imposed between borehole data and their neighbouring soundings. This is an approach that has been used successfully for 1D AEM inversion previously, in for example, laterally constrained inversion (Auken *et al.*, 2005), holistic inversion (Brodie and Sambridge, 2006; Brodie, 2010) and spatially constrained inversion (Viezzoli *et al.*, 2008). Christensen *et al.* (2009) use a different three-stage procedure where the soundings are inverted independently in stages one and three, but in the final stage lateral constraints that were derived in the second stage by a parameter correlations technique, are imposed.

We have developed a 1D AEM inversion algorithm that inverts multiple samples at once in order to take advantage of the lateral correlation of the geology and borehole conductivity log data. Of the aforementioned methods, our is most closely similar to spatially constrained inversion (Viezzoli *et al.*, 2008) since it inverts AEM data from soundings distributed across multiple flight lines, to a 1D conductivity model attached to each sounding. Rather than using a Voronoi tessellation to create a network of neighbouring soundings, across which lateral constraints are applied, our algorithm uses the concept of a search radius. Lateral constraints are applied by encouraging the individual layer conductivities of the 1D models to be as close as possible to the inverse distance weighted average of all neighbouring models that are within a specified search radius distance of itself. Borehole conductivity log data constraints are applied in a similar manner. We give the details of the formulation of the inverse problem and a real-data example of its application in the following sections.

METHOD AND RESULTS

Algorithm

Our inversion program is called *GALEIALLATONCE* because the central concept is to invert all the AEM soundings from a particular survey at once, with constraints from all borehole conductivity logs, in a single optimisation problem. Although, there are user options for choosing data subsets from a particular flight line, list of flight lines, or polygonal area(s). The spatial distribution of the AEM soundings and the boreholes may be arbitrary. Conceptually, there is an individual fixed thickness 1D conductivity model associated with or attached to every AEM sounding, with a fixed number, N_l, of layers.

In general there will be N_s soundings of AEM data to be inverted, which for an AEM system that has N_w windows (possibly in multiple transmitter moments), there will be $N_d = N_s \times N_w$ data to be inverted and stored in the column vector $\boldsymbol{d}^0$ with associated assigned errors stored in the vector $\boldsymbol{d}^e$. We solve for the model parameter vector, $\boldsymbol{m}$, which has length $N_m = N_s \times N_l$, and is made up of the logarithms of the conductivities (log-conductivity) of the layers of the individual 1D conductivity models attached to each AEM sounding.

The algorithm minimises the following penalty or objective function,

$$\Phi = \Phi_d + \lambda \Phi_m; \text{ subject to } \Phi_d \approx 1. \tag{1}$$

The penalty function is comprised of a data misfit term Φ_d, a regularisation parameter λ, and a model norm term Φ_m. The regularization parameter λ is used to tune the relative weights between the data misfit and model norm terms. In the current implementation, we manually set λ to a fixed value for all iterations. We expect to implement a line search method (e.g., Constable *et al.*, 1987). to automatically choose a suitable value for the regularisation parameter within each iteration in future improvements.

Data misfit (Φ_d)

The data misfit term,

$$\Phi_d = \frac{1}{N_d} \sum_{i=1}^{N_d} \left(\frac{g_i(m) - d_i^0}{d_i^e} \right)^2 = \left(g(m) - d^0 \right)^T W_d \left(g(m) - d^0 \right), \tag{2}$$

is a conventional error normalised L_2 measure of misfit between the observed data, $\boldsymbol{d}^0$, and the forward modelled data, $\boldsymbol{g}(m)$. The diagonal matrix, $\boldsymbol{W}_d = (1/N_d)[diag(\boldsymbol{d}^e)]^{-2}$ is the inverse noise covariance matrix normalised for the number of data, assuming independent Gaussian noise. The calculation of $\boldsymbol{g}(m)$ is a straight forward procedure of modelling the forward response of the conductivity model attached to each sounding. All forward modelling and analytic derivative calculations are carried out using the 1D AEM forward modelling routines described in Brodie (2010).

Model regularization norm (Φ_m)

The model regularization term,

$$\Phi_m = \Phi_r + \Phi_v + \Phi_h + \Phi_b, \tag{3}$$

is comprised of four terms ($\Phi_r, \Phi_v, \Phi_h, \Phi_b$), that impose different types of constraints or regularization on the model parameters, $\boldsymbol{m}$. The relative weights of the four regularization terms can be tuned by setting corresponding weights ($\alpha_r, \alpha_v, \alpha_h, \alpha_b$) on each term, as will become clear in the following equations.

Reference model constraints (Φ_r)

The reference model term,

$$\Phi_r = \frac{\alpha_r}{N_m} \sum_{i=1}^{N_m} \left(\frac{m_i - m_i^0}{m_i^e} \right)^2 = (m - m^0)^T W_r (m - m^0), \tag{4}$$

penalises discrepancy between m and a log-conductivity reference model, m^0. The reference model also serves as a starting model in the iterative inversion process. The vector m^e stores the uncertainties on the conductivity reference model values. The tuning factor α_r is a weight to tune the overall influence of the reference model constraints. Thus the diagonal matrix $W_r = (\alpha_r/N_m)[diag(m^e)]^{-2}$ is an inverse model parameter covariance matrix normalised for the number of reference model constraints and the tuning weight α_r.

Vertical roughness constraints (Φ_v)

The vertical roughness term,

$$\Phi_v = \frac{\alpha_v}{N_s} \sum_{i=1}^{N_s} \frac{1}{N_l - 1} \sum_{k=1}^{N_l - 1} \left(\frac{m_{i,k+1} - m_{i,k}}{[t_{i,k+1} + t_{i,k}]/2} \right)^2 = m^T V^T V\, m, \tag{5}$$

or alternatively,

$$\Phi_v = \frac{\alpha_v}{N_s} \sum_{i=1}^{N_s} \frac{1}{N_l - 2} \sum_{k=2}^{N_l - 1} \left(\frac{m_{i,k+1} - m_{i,k}}{[t_{i,k+1} + t_{i,k}]/2} - \frac{m_{i,k} - m_{i,k-1}}{[t_{i,k} + t_{i,k-1}]/2} \right)^2 = m^T V^T V m, \tag{6}$$

penalises the vertical roughness of the individual conductivity models. Here, $m_{i,k}$ and $t_{i,k}$ denote the log-conductivity and thickness of the kth layer of the model attached to the ith sounding respectively. The factor α_v is a weight to tune the overall influence of the vertical roughness constraints relative to the other regularization constraints. In Equation (5) the roughness norm is measured in terms of first derivatives, and V is a normalised first-finite-difference operator matrix (i.e., of the form $[\ldots \quad -1 \quad 1 \quad \ldots]$). In Equation (6) the roughness norm is measured in terms of second derivatives, and V is a normalised second-finite-difference operator matrix (i.e., of the form $[\ldots \quad 1 \quad -2 \quad 1 \quad \ldots]$). In both cases, the matrix V also absorbs the tuning weight and factors to normalise for the number of constraints, (i.e., $\sqrt{\alpha_v/(N_s \times [N_l - 1])}$ or $\sqrt{\alpha_v/(N_s \times [N_l - 2])}$). Note that the square-root is necessary to account for the $V^T V$ part of equations (5) and (6).

Lateral continuity constraints (Φ_h)

The lateral continuity term, Φ_h, is a measure of lateral continuity between the conductivity model associated with every sounding and the conductivity of the models at their neighbouring soundings. The measure compares the log-conductivity of each layer with the average log-conductivity over the same elevation (i.e., above sea level) range of all its neighbours. It is therefore not a smoothness constraint as such, but is probably best described as a *sameness* or *flatness* constraint.

The influence of each neighbour is weighed by an inverse distance to the power, p ,scheme. If we denote the sth sounding to have n_s neighbours that are within its search radius distance, a ,of itself, and that the distance between the sth and the tth soundings to be r_{st}, then we can define the normalised inverse distance to the power p weight that operates between the sth and the tth sounding to be,

$$w_{st} = \begin{cases} \left(\dfrac{1}{r_{st}}\right)^p \Big/ \sum_{k=1}^{n_s} \left(\dfrac{1}{r_{sk}}\right)^p, & r_{st} \leq a, \\ 0, & r_{st} > a \end{cases} \tag{7}$$

such that the weights sum to unity. To prevent large or infinite weights, if there happens to be extremely close or coincident soundings, if r_{st} is less than 10 m we set it to 10 m.
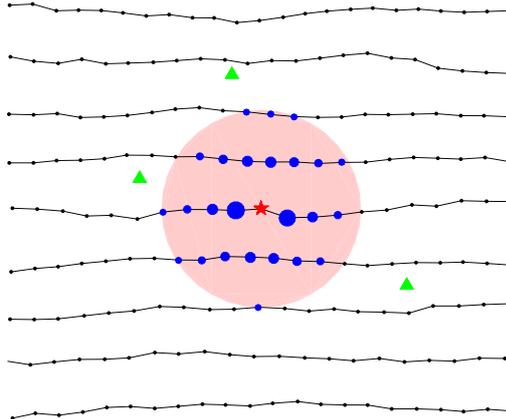

Figure 1: For a particular AEM sounding (red star), all neighbouring soundings (blue circles) within its' search radius (pale red shaded circle) contribute to that soundings lateral constraints. Here, the size of the blue circles indicates the weights for inverse distance to the power p=1.5 weighting. Green triangles represent borehole locations.

Since there will be topographic variation within the search radius, in general, we need to compare the conductivity of a layer attached to one sounding with multiple different layers attached to neighbouring soundings. To allow this, we first denote, v_{stkl} to be the fractional vertical overlap between the kth layer of the model attached to the sth sounding, and the lth layer of the model

attached to the tth sounding (see **Figure 2** for an explanation). Usually v_{stkl}, will be zero because any given layer in the sth model will not overlap with many layers in the tth model. The weighs v_{stkl} are described as a fraction overlap because they sum to unity for any pair of soundings st. We can now define the lateral continuity term to be,

$$\Phi_h = \frac{\alpha_h}{N_s} \sum_{s=1}^{N_s} \frac{1}{N_l} \sum_{k=1}^{N_l} \sum_{\substack{t=1 \\ t \neq s}}^{N_s} \sum_{l=1}^{N_l} \left[w_{st} v_{stkl} (m_{t,l} - m_{s,k}) \right]^2 = m^T H^T H\, m. \tag{8}$$

The normalised operator matrix H maps the model parameters, m, to a vector of differences between the model parameters, and the averages of the log-conductivity of the layers occupying the same elevation, in the models attached to neighbouring soundings, and weighted by their respective distances. The H matrix also absorbs the tuning weight and factors to normalise for the total number of lateral constraints (i.e., $\sqrt{\alpha_h/(N_s \times N_l)}$).
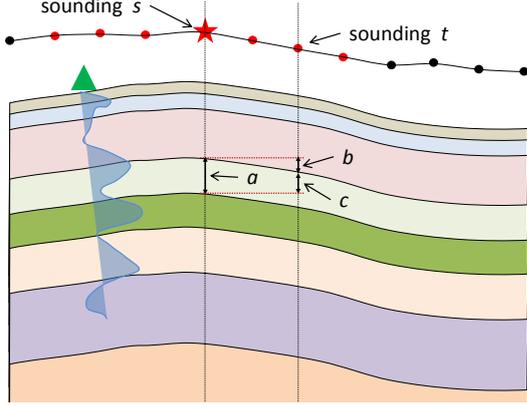

Figure 2: Illustration of how the fractional vertical overlap weights are calculated for the lateral constraint for sounding s and linking neighbour t. In Equation (8) the fractional overlap weights for layer 4 are $v_{st43} = b/a$ and $v_{st44} = c/a$.

Borehole conductivity log constraints (Φ_b)

The borehole conductivity regularization term, Φ_b, penalises discrepancy between the logarithm of downhole conductivity data and the log-conductivity of the models attached to its neighbouring soundings at the same elevation. Let there be N_b boreholes with conductivity logs to be considered as constraining information. For each borehole we segment the borehole conductivity log data into sections corresponding to the 1D model layer depths. We denote the average, of the measured log-conductivity, over the kth segment of the bth borehole log as $c_{b,k}^0$, to which we assign estimated noise c_{bk}^e. In general there will be $N_c \leq N_b \times N_l$, borehole constraints in total, because the conductivity logs will only intersect a subset of layers due to the limited depth of boreholes and any portions of the boreholes that cannot be logged.

Exactly analogous to Equation (7) we calculate a set of weights, w_{bt}, to weight Φ_b based on the distance between the bth borehole and the tth sounding. Similarly, analogous to Equation (8) we use the weight v_{btkl} that gives the fractional vertical overlap between the borehole conductivity log data associated with the kth segment in the bth borehole and the lth layer in the model attached to the tth sounding. The borehole conductivity regularization term is then defined as,

$$\Phi_b = \frac{\alpha_b}{N_c} \sum_{b=1}^{N_b} \sum_{k=1}^{N_l} \sum_{t=1}^{N_s} \sum_{l=1}^{N_l} \left[w_{bt} v_{btkl} \frac{m_{t,l} - c_{b,k}^0}{c_{b,k}^e} \right]^2 = \left(B\, m - c^0 \right)^T W_b \left(B\, m - c^0 \right). \tag{9}$$

Here W_b is the inverse noise covariance matrix of the segments of borehole data, assuming independent Gaussian noise, normalised for the total number of borehole data segments, and scaled by the tuning weight $W_b = (\alpha_b/N_c)[diag(c^e)]^{-2}$. The normalised operator matrix B maps m, to a vector of the average log-conductivities corresponding to each borehole data segment. The averages are over all the neighbouring soundings within the search radius of the borehole, weighted by their respective distances, and over the same elevation range as the data segment.
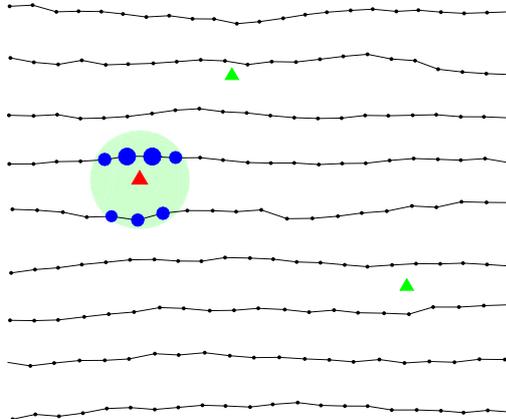
Linearized system of equations

To solve the non-linear inversion problem we use an iterative gradient based minimisation scheme to minimise the penalty function Φ. The solution vector is initialised to the reference model m^0. In the nth iteration we seek to update the current model m^n to an improved model m^{n+1} such that the revised data misfit, $\Phi_d^{n+1} \approx 0.7 \times \Phi_d^n$. We begin by substituting the matrix forms of Equations (2), (3), (4), (5) (or (6)), (8) and (9) into Equation (1) to yield,

Figure 3: For a particular borehole conductivity log (red triangle), all neighbouring AEM soundings (blue circles) within its' search radius (pale green shaded circle) contribute to that borehole log's lateral constraints. The size of the blue circles indicates the weights for inverse distance to the power p=1.5 weighting.

$$\Phi = \left(g(m) - d^0\right)^T W_d \left(g(m) - d^0\right)$$
$$+ \lambda \left[\left(m - m^0\right)^T W_r (m - m^0) + m^T V^T V m + m^T H^T H m + \left(Bm - c^0\right)^T W_b \left(Bm - c^0\right)\right]. \quad (10)$$

Using, the first order Taylor series approximation,

$$g\left(m^{n+1}\right) \cong g(m^n) + G^n\left(m^{n+1} - m^n\right) \quad (11)$$

where, G^n is the Jacobian matrix evaluated at m^n in model space, whose i,jth element is the partial derivative of ith predicted data with respect to the jth model parameter (i.e., $G_{ij}^n = \partial g_i(m^n)/\partial m_j^n$). After substituting m^{n+1} for m and making use of Equation (11), Equation (10) becomes,

$$\Phi = \left(g(m^n) + G^n\left(m^{n+1} - m^n\right) - d^0\right)^T W_d \left(g(m^n) + G^n\left(m^{n+1} - m^n\right) - d^0\right)$$
$$+ \lambda \left[\left(m^{n+1} - m^0\right)^T W_r \left(m^{n+1} - m^0\right) + m^{n+1}{}^T V^T V m^{n+1} + m^{n+1}{}^T H^T H m^{n+1}\right.$$
$$\left. + \left(Bm^{n+1} - c^0\right)^T W_b \left(Bm^{n+1} - c^0\right)\right]. \quad (12)$$

A minima of the penalty function is found by differentiating with respect to the new model parameters (m^{n+1}) and setting the result to zero, which yields,

$$\partial \Phi / \partial m^{n+1} = 2 G^n{}^T W_d \left(g(m^n) + G^n\left(m^{n+1} - m^n\right) - d^0\right)$$
$$+ \lambda \left[2 W_r\left(m^{n+1} - m^0\right) + 2 V^T V m^{n+1} + 2 H^T H m^{n+1} + 2 B^T W_b \left(Bm^{n+1} - c^0\right)\right] = 0. \quad (13)$$

After eliminating the 2s and collecting the terms involving the unknown vector m^{n+1} onto the left hand side Equation (13) becomes the linearized system of equations,

$$A m_{n+1} = b, \quad (14)$$

where,

$$A = G^n{}^T W_d G^n + \lambda[W_r + V^T V + H^T H + B^T W_b B], \quad (15)$$

and,

$$b = G^n{}^T W_d \left(d^0 - g(m^n) + G^n m^n\right) + \lambda[W_r m^0 + B^T W_b c^0]. \quad (16)$$

The linearized system in Equation (16) is solved using the preconditioned conjugate gradient method to yield the updated model vector m_{n+1}. We then predict the updated forward modelled data, $g(m^{n+1})$, and corresponding data misfit to make sure that $\Phi_d^{n+1}(m^{n+1}) < \Phi_d^n(m^n)$, Additionally, we apply step-length damping to find a step-factor $0 < u \leq 1$ such that, $\Phi_d\left(m_{step}^{n+1}\right) \cong 0.7 \times \Phi_d(m^n)$ where, $m_{step}^{n+1} = m^n + u(m^{n+1} - m^n)$ via a line search. This ensures that we only slowly converge to the solution, preventing too much unwarranted structure from entering into the model in the early iterations, that then becomes difficult to remove (Constable *et al.*, 1987). Upon finding a suitable value for the step-factor u, we set $m^{n+1} = m_{step}^{n+1}$ and proceed to the next iteration. The main non-linear iteration loop continues until either: $\Phi_d \cong 1$; the percentage achieved improvement in the data misfit Φ_d is less than a user defined percentage (e.g., 1%); or a maximum number of iteration is exceeded (e.g., 50).

Computations

The program code is fully parallelized for execution on a high performance distributed memory cluster computer or on a multi-core shared memory workstation using the MPI standard (Message-Passing-Interface-Forum, 1994). All the matrices in the algorithm are sparse and well suited to scalable operations, since they are stored in distributed compressed spare row fashion. We use the open-source software library PETSc (Balay *et al.*, 2014) to handle all of the matrix storage and linear algebra requirements, including the conjugate gradient solver. To save memory, the more dense linear system matrix, A in Equation (14), is never actually explicitly stored, instead the component matrices (G, V, H, B etc.) are stored and the matrix-vector products $b = Ax$ are computed on the fly as required by the conjugate gradient algorithm,

The software is accessible as C++ source code which is packaged in a Git code repository and may be downloaded from Geoscience Australia's ga-aem repository on GitHub® at https://github.com/GeoscienceAustralia/ga-aem. The code can be compiled using most modern C++ compilers on both Linux and Windows® based systems. In due course we also expect to make the algorithm available as a service on the Australian National Virtual Geophysics Laboratory (ANVGL) portal (http://www.anvgl.ga.gov.au).

EXAMPLE

To demonstrate the results of the new algorithm we inverted SkyTEM data that were acquired in 2009 as part of the Broken Hill Managed Aquifer Recharge (BHMAR) project (Lawrie *et al.*, 2012). The BHMAR survey consisted of a total of 32,659 line kilometres of data acquired at 200 m line spacing and with a nominal 30 m transmitter/receiver frame height above ground level. We chose to invert a 3,700 line kilometre subset of the BHMAR data that is centred upon the Menindee AEM Calibration Range, which is currently being established by Geoscience Australia, near the township of Menindee, New South Wales. The calibration range is an area where there is a good concentration of boreholes with downhole conductivity logging and other ancillary ground based geophysical data. We inverted the data with our new all-at-once (AAO) program called GALEIALLATONCE, as well as with our conventional deterministic sample-by-sample (SBS) inversion program called GALEISBSTDEM (Brodie and Richardson, 2015) to facilitate comparison.

Both the SBS and AAO inversions were run with identical data and noise settings. The low- and high-moment Z-component SkyTEM data were inverted together. The assigned noise levels were 3.6% relative error plus an absolute noise floor, which ranged from 5.78×10^{-11} V/Am^4 for the earliest time low-moment window to 3.57×10^{-14} V/Am^4 for the latest high-moment time window. The subset area contained 161201 soundings, spaced approximately 23 m apart to 1D conductivity models discretised into 30 layers. The 1D models all had a thickness of 0.5 m for the top layer, increasing to 31.2 m for the penultimate layer before the halfspace.

Since each dual-moment SkyTEM sounding had 19 low-moment and 21 high-moment windows for this specific survey, the AAO inversion had 6.4 million data and 4.8 million model parameters to solve for. There were 90 downhole conductivity logs in the subset area that were included as constraints in the AAO inversion, to which we assigned 10% relative error. Some of the logs were in clusters of nested boreholes, and were therefore quite close to each other. We set the search radius to 1,000 m for lateral constraints (see **Figure 1**), and 250 m for borehole constraints (see **Figure 3**). Both inversions used a homogeneous 0.050 S/m conductivity reference model. **Figure 4** and **Figure 5**.show the inversion results for 18 km portions of the two particular flight lines (22870 and 23310), which are coincident with the two Menindee AEM Calibration Range lines.
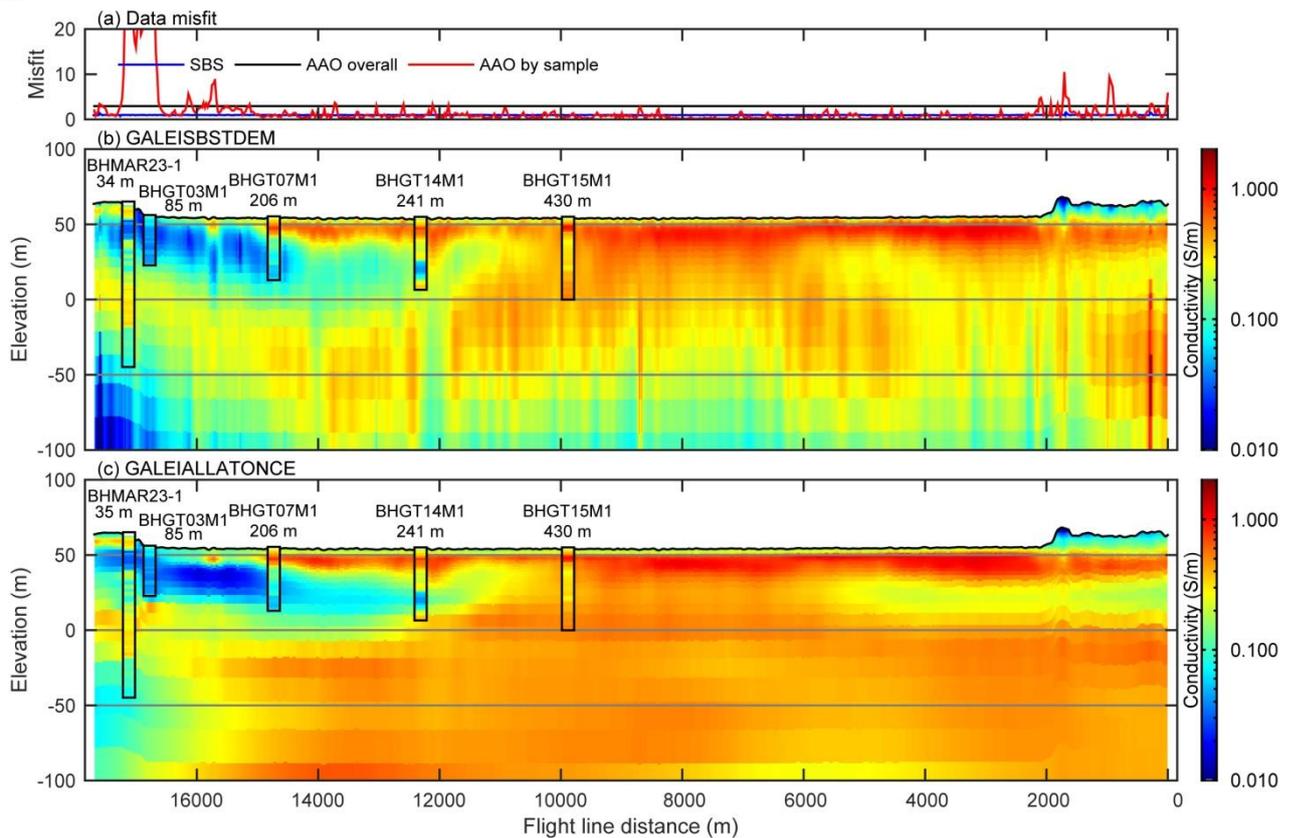

Figure 4: Comparison conductivity sections for flight line 22870 showing: (a) the data misfits for both inversions; (b) section for the conventional stitched sample by sample (SBS) inversion GALEISBSTDEM; and (c) section for the new all-at-once (AAO) inversion GALEIALLATONCE. The five adjacent borehole conductivity logs are superimposed on the sections with the same colour lookup table, along with their respective distance from the flight line.

On **Figure 4** and **Figure 5**, the top panels (a) show the final data misfits that were achieved. The SBS inversion (blue trace) typically reached the expected normalised misfit $\Phi_d \approx 1.0$ for every individual sounding. The AAO inversion, however

reached an overall misfit (black trace) of $\Phi_d = 2.93$ in iteration 14, after which the algorithm finishes because the misfit could no longer be improved. The AAO inversion also calculates and outputs a data misfit for each individual sounding (red trace). It can be seen that the individual AAO by sounding misfit is typically close to the desired level of 1.0, but is also often very high on some soundings. These outliers bias the overall misfit and prevent further convergence.

On **Figure 4** and **Figure 5**, the second panels (b) show the conductivity sections from the SBS inversion and panel (c) shows the conductivity section from the AAO inversion. The sections also have adjacent (within 500 m of the flight line) conductivity logs superimposed with the same colour lookup table. The respective distances between borehole and flight line are also shown. It is immediately clear on both figures that the AAO inversion is more geologically plausible than the SBS inversion because it does not contain the vertical striping and the artefacts toward the bottom of the section. The AAO inversion sections are more coherent in nature and the apparent stratigraphic layering appears more contiguous. Furthermore the AAO inversion matches the conductivity logs better than the SBS inversion, as would be expected since the logs were included as constraints in the AAO inversion only.

It can be seen that in most places where there are larger spikes in the AAO inversion individual sample data misfit (red traces on panel a), there are corresponding artefacts in the SBS inversion conductivity section. Our interpretation of this is that these soundings have higher than the usual noise (compared to our assigned noise levels), which the SBS inversion chases, and is still able to (over-)fit the data with an inferior model. Whereas, since the AAO inversion is laterally constrained it is not free to chase the noise. Instead it averages through the noise and produces a more plausible model. In these places the AAO appears not to fit the data locally, however, nor should it if those soundings do possess more noise than those assigned in the inversion.

Also, our assessment is that the deeper parts of the sections (below ~0 m elevation) are likely to be more correct in the AAO inversion. In this conductive terrain, the sensitivity of the data to the conductivity of layers below ~70 m depth is diminished because of the diffusive nature of EM methods, and the SBS inversion results tend to be heavily influenced by sounding-to-sounding noise and/or non-uniqueness.
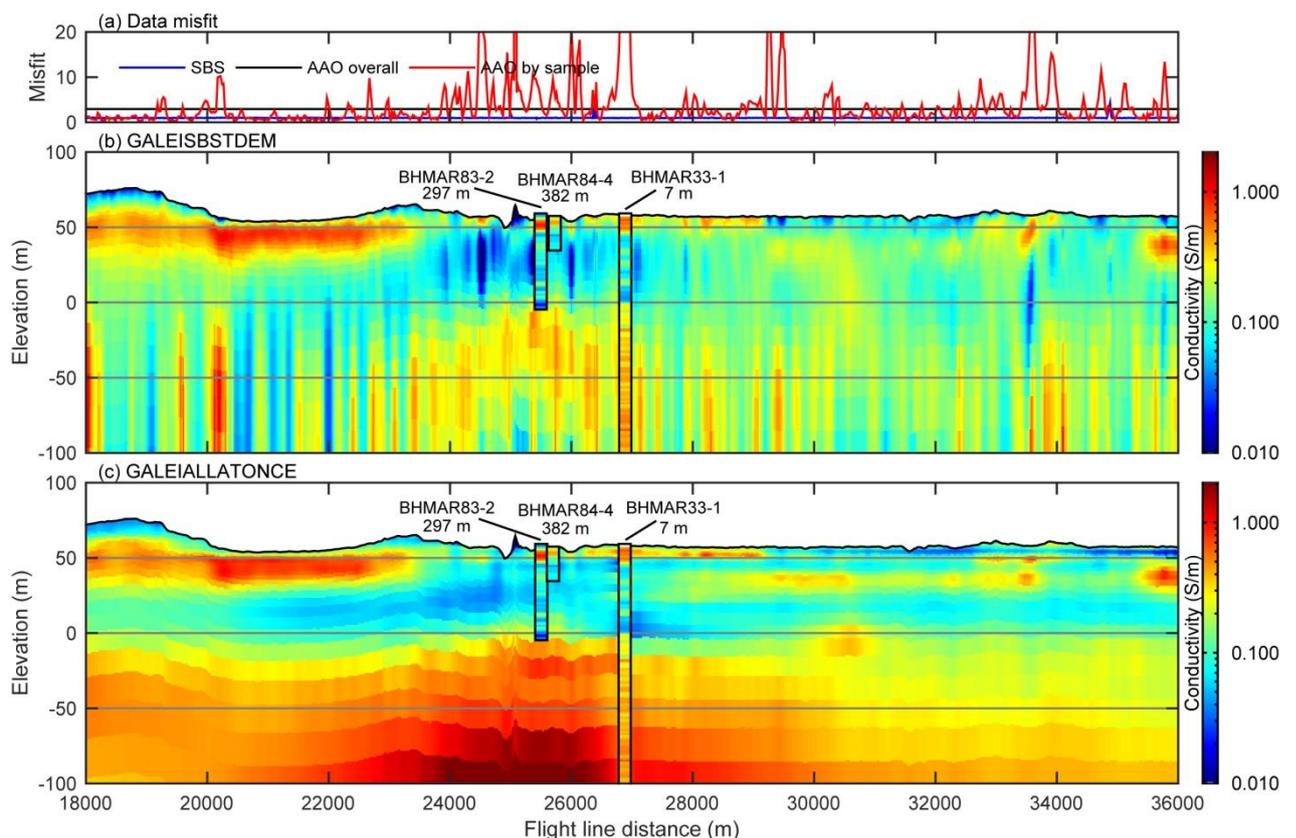

Figure 5: Comparison conductivity sections for flight line 23310 showing: (a) the data misfits for both inversions; (b) section for the conventional stitched sample by sample (SBS) inversion GALEISBSTDEM; and (c) section for the new all-at-once (AAO) inversion GALEIALLATONCE. The three adjacent borehole conductivity logs are superimposed on the sections with the same colour lookup table as the AEM conductivity section, along with their respective distance from the flight line.

CONCLUSIONS

Our new all-at-once inversion algorithm is an intuitive and effective way to imposing lateral constraints that encourage similarity between neighbouring AEM soundings, which cannot be achieved in conventional independent sample-by-sample stitched 1D inversion. It also provides a mechanism for incorporating borehole conductivity log data as a hard constraint rather than a soft regularization constraint.

We have demonstrated that our new algorithm produces a superior conductivity model compared to our conventional sample-by-sample algorithm. This is in terms of how well the conductivity models match borehole data, as well as the coherency of the resultant sections. By including borehole data, non-uniqueness is reduced at least in the vicinity of the boreholes, but this is extended further afield by virtue of the lateral constraints. The algorithm tends to suppress the effect of localised sounding-to-sounding noise, which when coupled with non-uniqueness, results in artefacts in conventional conductivity sections. The lateral constraints prevent overfitting of the localised noise, by in-effect fitting through it. The more coherent models, which also match the borehole data, ultimately lead to more geological plausible and interpretable conductivity sections.

A potential risk with using lateral constraints is that, if they are too tight, short-wavelength real anomalies, caused for example by discrete conductors, may not be fitted and thus would not appear in the resultant conductivity sections. Accordingly we would encourage that the method be used alongside conventional sample-by-sample inversion algorithms. A further pitfall that can occur when large groups of soundings are inverted simultaneously, is that the occasional extremely noisy sounding or areas where the geology is not 1D, can prevent the inversion from converging. As part of future improvements, we expect to implement the $L1$ norm instead of the $L2$ norm for the data misfit term to help remedy this.

ACKNOWLEDGMENTS

REFERENCES

Auken, E., Christiansen, A. V., Jacobsen, B. H. and Foged, N., 2005. Piecewise 1D laterally constrained inversion of resistivity data. *Geophysical Prospecting* **53**, 497-506.

Balay, S., Adams, M. F., Brown, J., Brune, P., Buschelman, K., Eijkhout, V., Gropp, W. D., Kaushik, D., Knepley, M. G., McInnes, L. C., Rupp, K., Smith, B. F. and Zhang, H., 2014. PETSc Web Page. Online: http://www.mcs.anl.gov/petsc.

Brodie, R. and Sambridge, M., 2006. A holistic approach to inversion of frequency-domain airborne EM data. *Geophysics* **71(6)**, G301-G312.

Brodie, R. C., 2010. Holistic inversion of airborne electromagnetic data. Australian National University, Canberra. Ph.D. Thesis. Online: http://hdl.handle.net/1885/49403.

Brodie, R. C. and Richardson, M., 2015. Open Source Software for 1D Airborne Electromagnetic Inversion. *ASEG Extended Abstracts* **2015(1)**, 1-3.

Christensen, N. B., Reid, J. E. and Halkjær, M., 2009. Fast, laterally smooth inversion of airborne time-domain electromagnetic data. *Near Surface Geophysics* **7(5)**, 599-612.

Constable, S. C., Parker, R. L. and Constable, C. G., 1987. Occam's inversion; a practical algorithm for generating smooth models from electromagnetic sounding data. *Geophysics* **52(3)**, 289-300.

Lane, R., Brodie, R. C. and Fitzpatrick, A., 2004. Constrained inversion of AEM data from the Lower Balonne area, Southern Queensland, Australia. *Open file report*, 163, Cooperative Research Centre for Landscapes, Environment and Mineral Exploration. Online: http://crcleme.org.au/Pubs/OPEN%20FILE%20REPORTS/OFR%20161-162-163-164-166-167/OFR163.pdf.

Lawrie, K. C., Brodie, R. S., Tan, K. P., Gibson, D., Magee, J., Clarke, J. D. A., Halas, L., Gow, L., Somerville, P. and Apps, H. E. (ed), 2012. BHMAR Project: Data acquisition, processing, analysis and interpretation methods. Geoscience Australia, Canberra. **Record 2012/11**, 782 pp. Online: https://d28rz98at9flks.cloudfront.net/73819/Rec2012_011.pdf.

Message-Passing-Interface-Forum, 1994. MPI: A message-passing interface standard. *International Journal of Supercomputing Applications* **8(3-4)**, 165-416.

Viezzoli, A., Christiansen, A. V., Auken, E. and Sorensen, K., 2008. Quasi-3D modeling of airborne TEM data by spatially constrained inversion. *Geophysics* **73(3)**, F105-F113.